

# Complexation of Gas-Phase Metal Ions with Furan: Experimental and Quantum Chemical Binding Energies

Ronald L. Grimm, John B. Mangrum, and Robert C. Dunbar\*

Department of Chemistry, Case Western Reserve University, Cleveland, Ohio 44106

Received: July 1, 2004; In Final Form: October 1, 2004

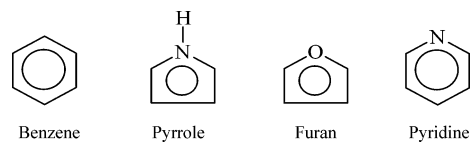
Binding of metal ions to furan in the gas phase to form  $M^+(\text{furan})$  complexes was studied by radiative association kinetics (RAK) in the Fourier transform ion cyclotron resonance (FT-ICR) spectrometer, and by density functional theory (DFT) calculations of the structures and binding energies. Three main-group metals and the first-row transition metal series were included. Binding energies were compared with previous studies of cation- $\pi$  binding to the aromatic  $\pi$  face involving benzene and pyrrole ligands. It was found that furan is a somewhat weaker  $\pi$ -binding ligand than benzene for all of the metal ions (by an amount of the order of 5 kcal mol<sup>-1</sup>), in contrast to pyrrole, which is stronger than benzene in most cases. This was rationalized as a largely electrostatic effect. Furan presents the competing possibility of metal-ion binding to the oxygen, but it was found that the oxygen binding site has lower affinity than the  $\pi$  site for all metal ions. The preference for the  $\pi$  site is of the order of 6 kcal mol<sup>-1</sup> for metal ions without active d electrons, and of the order of 20 kcal mol<sup>-1</sup> for the transition metal ions with partially filled d-orbital shells. A quantitative model was developed and applied to separate out the electrostatic contributions to ion/ligand interaction from other types of interactions.

## Introduction

Cation- $\pi$  binding between metal ions and cyclic  $\pi$  ligands has been interesting from several points of view. As one of the fundamental modes of interaction between metal ions and organic molecules, it is widely relevant to understanding metal complexation to molecular substrates, to graphitic surfaces, and to the more diverse surface landscapes offered by extended systems such as polypeptides and polynucleotides. The cation- $\pi$  binding idea has attracted wide interest as a likely structure-organizing principle in large-scale biological structures<sup>1</sup> and host-guest situations.<sup>2</sup> Since a complex surface often offers binding sites of more than one type, it is useful to make binding studies with model compounds having a choice of binding sites, to characterize the competition (or cooperation) of binding between sites of various types. Several studies by our group have been directed at understanding the competition of metal ion binding between  $\pi$  sites and n-donor basic sites involving oxygen or nitrogen.

The furan ligand is an interesting one in this context of competing binding sites, offering the possibility of cation- $\pi$  binding on the face of the aromatic ring, or lone-pair binding to the exposed oxygen on the edge of the ring. Furan also rounds out the study of a series of ligands of particular interest for understanding the essentials of cation- $\pi$  binding of metal ions, namely, benzene, pyrrole, furan, and pyridine. This is a series of simple cycles with full 6-electron  $\pi$  aromaticity, differing in the character of ring heteroatom substitution by N or O.

Benzene, the prototypical reference system for this comparative series, has its six-electron  $\pi$  system constructed from one electron from the  $p_z$  orbital of each carbon (within an  $sp^2$  hybridization picture). For both pyrrole and furan, two of the six  $\pi$  electrons are contributed by a pair of electrons in the  $p_z$



orbital of the heteroatom. For pyrrole this participation in the  $\pi$  system, along with the three  $\sigma$  bonds, exhausts the five valence electrons of the N atom. For furan, an in-plane lone pair of electrons, along with the two electrons contributed to the  $\pi$  system via the oxygen  $p_z$  orbital and the two  $\sigma$  bonds, completes the assignment of the six valence electrons of the O atom. Pyridine has only one of its six  $\pi$  electrons contributed by the nitrogen  $p_z$  orbital, and also, analogous to furan, has an in-plane lone pair of electrons on the N atom. All four of these molecules have similar possibilities of cation- $\pi$  binding with a cation sitting in the electrostatic potential energy well above the ring, which can involve the metal d orbitals (filled and empty) interacting with the  $\pi$  and  $\pi^*$  orbitals of the aromatic ring. In addition, furan and pyridine have the possibility of in-plane binding of the metal ion on the heteroatom lone pair. (Pyrrole has a binding site of electrostatic character on the nitrogen, which is calculated to be competitive for binding of purely electrostatic binders such as the alkali ions.<sup>3</sup> However, this binding is different from, and weaker than, the true n-donor basic sites offered by the exposed lone pairs of furan and pyridine.) The similarities and differences in the binding of metal ions, in particular transition metal ions, with these four ligands provide an interesting and valuable comparative study. Although the other three have been carefully studied, furan remains as a ligand whose systematic binding to metal cations has yet to be considered in detail.

Although pyridine can be considered as a member of this series of potentially  $\pi$ -binding simple heteroaromatic ligands, it is actually not a useful subject of study from the present point of view, because it does not appear to exhibit stable cation- $\pi$  binding. Calculations have indicated that the in-plane lone pair

\* To whom correspondence should be addressed. Phone: 216-368-3712. Fax: 216-368-3006. E-mail rcd@po.cwru.edu.

binding site is the only stable site,<sup>4</sup> and that metal ions initially located in a ring-binding geometry move spontaneously, apparently without significant barrier, into the nitrogen in-plane binding site. Accordingly, pyridine will not be considered further here.

Acting as an oxygen-donor ligand, furan is relatively weak, as shown for example in a recent structure<sup>5</sup> displaying an exceptionally long Zr–O bond in a zirconium complex having a furan geometrically constrained to oxygen-donor interaction with the metal. That furan is a weaker n-donor ligand than pyridine was also indicated in a binding study comparing a furan-containing macrocyclic ligand with a corresponding pyridine-containing ligand.<sup>6</sup> The furan system as a  $\pi$ -bonding ligand seems not to have been characterized in the condensed phase, although it seems likely that it could be tethered, constrained, and characterized in a  $\pi$ -bonding configuration just as has been done with other simple aromatic ligands.<sup>2,7,8</sup> Studying the competition between binding sites in model compounds such as furan in the gas phase is still limited by the lack of structure-sensitive gas-phase techniques, although spectroscopic tools are beginning to be available for addressing such questions.<sup>9–12</sup> For the most part, the comparison of binding sites on such ligands is limited to computational study, as was done in the present work.

The interesting question to address by computation is the relative metal-ion affinities of the two binding sites on furan. The ability of DFT calculations to compare ring  $\pi$  and oxygen lone-pair binding sites was considered in a recent computational study of metal-ion binding to phenol, benzene, and water.<sup>13</sup> Most important in the present context, the popular B3LYP functional was found to underestimate the metal ion affinity of the ring site compared with the oxygen site, whereas the MPW1PW91 functional gave an overall satisfactory comparison of the two types of sites. A further instance of a valid comparison of  $\pi$ -donor sites was provided in a spectroscopic characterization of the Cr<sup>+</sup>/aniline complex by infrared multiphoton dissociation, using a free-electron laser source.<sup>9</sup> The experiments showed the structure of the complex to be predominantly ring bound, confirming the prediction by DFT/MPW1PW91. These computational and experimental results give us confidence that the comparison of  $\pi$ -donor and n-donor sites by DFT/MPW1PW91 is credible.

Several experimental approaches have been applied to measuring gas-phase binding energies of metal-ion/ligand complexes. These include ligand exchange equilibrium,<sup>14</sup> ligand attachment equilibrium,<sup>15</sup> ion–molecule reaction bracketing,<sup>16</sup> photodissociation,<sup>17</sup> threshold collision-induced dissociation,<sup>18</sup> competitive collision-induced dissociation,<sup>19</sup> and radiative association kinetics (RAK).<sup>20</sup> The RAK approach used in the present experimental work has been found to be a useful way of extracting thermochemical information from the metal–ligand association reactions observed in the low-pressure environment of the Fourier transform ion cyclotron resonance (FT-ICR) cell. It is not as accurate and reliable as favorable applications of other approaches, but it is complementary in that it approaches the complex from the separated-reactants side as opposed to looking at dissociation of the preformed complex, and it has been found useful for comparing bond energies among similar systems. Applications of this approach to metal-ion binding systems have been Al<sup>+</sup> with benzene,<sup>21,22</sup> Cr<sup>+</sup> with fluorinated benzenes,<sup>23</sup> and MX<sup>+</sup> with benzene (where M is a metal and X is a halogen atom).<sup>24,25</sup> Recently this approach was applied in the study of M<sup>+</sup> with pyrrole, to which the present study provides a complementary companion.<sup>3</sup> We can also note a more

recent study of alkali ion binding to pyrrole by threshold collision-induced dissociation and HF/MP2 computation,<sup>26</sup> providing experimental information for the first time about the Na<sup>+</sup>/pyrrole system, which was only studied computationally in ref 3.

With respect to the furan ligand, scattered experimental binding information is available. Nanayakkara and Freiser<sup>27</sup> used both threshold photodissociation and reactive bracketing approaches on the Co<sup>+</sup>/furan complex. Including experimental uncertainties, their photodissociation results, supported by competitive CID observations on the Co<sup>+</sup>(furan)(NH<sub>3</sub>) complex, indicated an upper limit of 60 kcal mol<sup>-1</sup>. Furthermore, threshold photodissociation and ligand exchange bracketing both indicated that Co<sup>+</sup> binding is weaker to furan than to pyrrole. They interpreted the photodissociation threshold as giving a lower limit of 54 kcal mol<sup>-1</sup>, but threshold photodissociation is not a reliable way of determining such lower limits, and this value must be considered with caution. Su and Yeh<sup>28</sup> used a threshold photodissociation approach to give a value of 28.1 kcal mol<sup>-1</sup> for the Ag<sup>+</sup>(furan) binding energy, but this threshold-derived value must be considered more as an upper limit than as an actual value. In a similar study,<sup>29</sup> this same group assigned an upper limit of 37 kcal mol<sup>-1</sup> for the Cu<sup>+</sup>(furan) binding energy. Bakhtiar and Jacobson used ligand displacement bracketing to place the binding energy of Fe<sup>+</sup>(furan) between 38.5 and 60 kcal mol<sup>-1</sup>.<sup>30</sup>

For the Ni<sup>+</sup>/furan system, a study by Kappes and Staley<sup>31</sup> provided thermochemical information relevant to the present work. Their investigation of ligand-exchange equilibria of NiL<sub>2</sub><sup>+</sup> complexes placed furan on a scale of free energies of NiL<sup>+</sup>–L bonds for about 50 molecules, from which bond enthalpies of the NiL<sup>+</sup>–L bonds were derived. Although it is not strictly accurate to use such second-ligand bond strengths to infer first-ligand binding energies, nevertheless this should give a good way to estimate relative Ni<sup>+</sup>–L values between closely related systems. Kappes and Staley<sup>31</sup> incorrectly considered furan to be an oxygen-basic ligand, but this had no effect on their thermochemical determination. Their results led to estimates of the Ni<sup>+</sup>/furan binding energy through several chains of comparison. The best comparison from their study is between furan and benzene, which indicated a furan binding free energy 8 kcal mol<sup>-1</sup> lower than that of benzene. Entropy effects should be similar for these two ligands, giving an enthalpy differential also of 8 kcal mol<sup>-1</sup>. Using a binding energy for benzene of 58 kcal mol<sup>-1</sup>,<sup>32</sup> this leads to an assignment of the Ni<sup>+</sup>/furan binding energy as 50 kcal mol<sup>-1</sup>. A confirmation of this within the Kappes and Staley study was provided by the comparison of the second-ligand binding thermochemistry of furan versus acetylene. Anchored to a Ni<sup>+</sup>/acetylene value of 45 kcal mol<sup>-1</sup> of Surya et al.,<sup>33</sup> this gives a Ni<sup>+</sup>/furan enthalpy estimate of 48 kcal mol<sup>-1</sup>. Entropy corrections are less secure in this latter comparison, and we consider the best estimate of the furan binding energy, as derived from this study, to be the value of 50 kcal mol<sup>-1</sup> based on the benzene comparison.

The RAK approach in the present work exploits the fact that the gas-phase association reaction between an ion and a neutral, such as, in the present study,



is highly sensitive to the energy of binding of the association product ion. Under very low-pressure conditions, where the product ion is stabilized by the emission of infrared photons, kinetic modeling can account for the effects on the reaction rate constant of the chemical nature of the reactants, and of the

structure, size, vibrational frequencies, and infrared emission intensities of the association complex. The remaining unknown quantity, the binding energy, can then be obtained by fitting the observed rate constant of reaction 1 to the kinetic model. Schemes for applying this strategy in both an approximate semiquantitative way<sup>34</sup> and a more detailed and quantitative way<sup>22</sup> have been described, and form the basis for thermochemical applications of this approach.

## Methods

**Experimental Details.** The RAK experiments were performed on a modified Nicolet FTMS-2000 spectrometer with a 3 T superconducting magnet,  $10 \times 5 \times 5 \text{ cm}^3$  cell, and IonSpec data system (more fully described in ref 23). The dual-region Nicolet vacuum chamber was pumped by a 1000 L/s Asti-Cryogenics cryopump on the low-pressure side and a 100 L/s Alcatel diffusion pump on the high-pressure side. The ICR cell was located on the low-pressure side, and the furan vapor was leaked from the high-pressure side, through the conductance limit aperture, into and through the cell region. Base pressures in the low-pressure region were measured below  $1 \times 10^{-9}$  Torr.

Pressures were measured with a Bayard-Alpert ionization gauge. The pressure of furan was corrected by an estimated ionization gauge factor.<sup>35</sup> Uncertainty in the reactant pressure was of concern because this is the main contributor to the rate constant uncertainty. Since the pumping geometry was identical with that used in the pyrrole study of ref 3, and since the ionization characteristics of furan and pyrrole are quite similar, it was expected that the absolute pressure calibration of the ionization gauge readings that was determined in that work should be valid within the same 30% uncertainty for the present measurements.

Furan (99+%) was used as purchased from Acros Organics. After multiple freeze–pump–thaw cycles to remove dissolved gases, it was introduced into the high-vacuum chamber through a Varian leak valve located on the high-pressure side of the vacuum system. Pressures of reactant vapor were typically  $5 \times 10^{-8}$  Torr.

The precursor metal ions were generated by a pulsed YAG laser (532 nm) focused on a metal target mounted on the solid probe tip. Thermalization of ions was achieved through collisions with furan, followed by isolation of the metal ions of interest by using ICR ejection techniques to remove unwanted ions. The intensities of the metal ion and the corresponding complexes were monitored as a function of reaction time in order to derive the association rate constant.

The reduction of the measured association rate constants to binding energies was carried out in fashion similar to that described in detail in ref 3. The required infrared frequencies and radiative intensities of the  $M^+$ (furan) complexes were taken from the DFT calculations (basis set “A”), with a scaling factor of 0.95 for the frequencies.<sup>9</sup> The kinetic modeling used the variational transition state theory (VTST) approach,<sup>3,36</sup> which is the most detailed and theoretically justifiable approach available for these modeling calculations.

The existence of low-lying excited electronic states of the complexes has a small effect on the modeled kinetics. Since these excited states were not calculated in detail for the furan systems, the corrections used for the corresponding pyrrole systems were applied.<sup>3</sup> Only for the  $\text{Fe}^+$  cases is the excited-states correction ( $3 \text{ kcal mol}^{-1}$ ) not negligible relative to the other sources of uncertainty in these determinations, and even there this is not an important contribution to our estimated uncertainty. As previously noted, the major uncertainty in the

calculation of the  $\text{Fe}^+$  affinities arises from the fact that this association (unlike all of the other metal ions in this series) involves a spin change, from the sextet free iron atom to the quartet ground state of the complex ion. Current DFT methods are not accurate in relating the energies of these different spin manifolds. As was done in the pyrrole system,<sup>3</sup> the present calculation was carried out by calculating the spin-conserving quartet-to-quartet binding energy by DFT, and then correcting this value by using the experimentally measured sextet-to-quartet excitation energy of the free iron ion ( $5.7 \text{ kcal mol}^{-1}$ ).

**Computational Details.** Density functional theory (DFT) provides a good combination of reasonable accuracy and computational tractability for transition metal complexes, and was used in the present calculations. Our experience with calculations to compare  $\pi$  binding sites with n-donor-base sites, in particular the study of phenol,<sup>13</sup> has suggested that the MPW1PW91 hybrid functional gives a better comparison of these different binding sites than the popular B3LYP hybrid functional, and at the same time gives absolute binding energy values agreeing with experimental points about as well as those calculated with B3LYP. This advantage was considered decisive for the present study, and the MPW1PW91 functional was used here consistently. This makes it slightly more difficult to compare the present results with the comparable study of pyrrole complexes which used B3LYP,<sup>3</sup> in view of the observation that MPW1PW91 gives  $\pi$ -cation binding energies of transition metal ions systematically higher than the corresponding B3LYP values by 1 to 5  $\text{kcal mol}^{-1}$ . Rather than going back to recalculate all of the pyrrole systems with the present protocol, comparability of the two studies was achieved as discussed below by using benzene as a common comparison standard for calculations with the two functionals.

It is characteristic of DFT methods that results with relatively small basis sets can be nearly as accurate and reliable as those with very large basis sets. Experience suggests that comparisons are stable and valid with modest bases which include adequate polarization and diffuse functions. Following our satisfactory experience in the calculation of phenol complexes,<sup>13</sup> the basis from that study, which will be called the “A” basis, was used in the present work for geometry optimizations and vibrational frequencies, consisting of 6-311+g(d) on the metal and 6-31+g(d,p) on other elements. Energy calculations were carried out with two larger basis sets, so that the effect of basis set expansion could be seen systematically. The first of these, the “B” basis, was 6-311+g(d,p) on all elements; the second, the “C” basis, used more extensive polarization functions and consisted of 6-311+g(2df,2pd) on all elements. Several trials with geometry optimization at the level of the “B” basis gave geometries indistinguishable from those from the “A” basis, so the latter was used for optimization of all the geometries reported here. The GAUSSIAN 98 computational package<sup>37</sup> was used for all calculations.

In line with what Stöckigt found in his systematic survey of basis set effects in  $\text{Al}^+$ /benzene,<sup>38</sup> it was found here that the increased polarization of the large “C” basis set gave a small but consistent increase in the computed cation- $\pi$  binding energies compared with the “A” and “B” bases (which gave essentially identical binding energies). For the ring-bound furan species, as seen in Table 1, this increase was of the order of 1.0 to 1.5  $\text{kcal mol}^{-1}$ . For the O-bound structures, where the binding involves more localized orbitals, one might expect less advantage in adding additional polarization functions to the basis, and indeed there was at most a very minor increase in binding energies in going from the “B” to the “C” basis (Table

**TABLE 1: Computed Binding Energies to Furan<sup>a</sup>**

	Na	Mg	Al	Sc	Ti	V	Cr	Mn	Fe <sup>b</sup>	Co	Ni	Cu
						ring bound						
BE (A)	17.9	26.9	28.1	43.0	44.8	42.1	31.5	26.6	39.8	47.2	51.1	45.9
BE (B)	17.9	26.7	28.1	42.6	44.3	42.1	31.5	26.6	39.6	47.1	50.9	45.7
BE (C)	19.1	28.3	30.2	44.4	46.2	43.5	32.8	28.0	40.7	48.2	52.2	46.9
						O bound						
BE (A)	16.8	24.5	21.7	33.0	28.5	28.9	26.0	21.7	23.5	32.4	31.1	32.7
BE (B)	15.3	24.9	22.0	33.4	28.8	29.3	26.4	22.1	23.8	32.8	31.4	33.1
BE (C)	15.3	25.6	22.6	33.5	28.9	29.6	26.7	22.3	24.2	33.2	31.7	33.4

<sup>a</sup> DFT/MPW1PW91, basis sets “A”, “B”, and “C” as described in the text, with individual ZPVE and average BSSE corrections (geometries optimized at the level of basis set “A”) (kcal mol<sup>-1</sup>). <sup>b</sup> For Fe<sup>+</sup> evaluations, the spin-conserving quartet–quartet association was calculated at the indicated level, and then the energy was corrected for the Fe<sup>+</sup> quartet–sextet excitation energy by subtracting 5.7 kcal mol<sup>-1</sup>.

**TABLE 2: Experimental Results and Computed Binding Energies Compared for Furan and Pyrrole<sup>a,b</sup>**

metal	binding energy					
	<i>k</i> <sub>RA</sub>		experiment (VTST)		theory (DFT)	
	furan	pyrrole	furan (±15%)	pyrrole	furan MPW1PW91	pyrrole B3LYP
Cr <sup>+</sup>	6 × 10 <sup>-15</sup>	4.5 × 10 <sup>-12</sup>	27	43	33	41
Fe <sup>+</sup>	1.6 × 10 <sup>-11</sup>	1.0 × 10 <sup>-10</sup>	48	54	46	49
Co <sup>+</sup>	2 × 10 <sup>-10</sup>	1.3 × 10 <sup>-9</sup>	61	>66	48	55
Ni <sup>+</sup>	2 × 10 <sup>-10</sup>	1.6 × 10 <sup>-9</sup>	59	>68	52	61
Cu <sup>+</sup>	8 × 10 <sup>-11</sup>	3.8 × 10 <sup>-10</sup>	56	59	47	58

<sup>a</sup> Pyrrole results from ref 3. <sup>b</sup> Rate constants in molecules cm<sup>-3</sup> s<sup>-1</sup>, energies in kcal mol<sup>-1</sup>.

1). Thus using the larger “C” basis set leads to a slight increase, of the order of 1 kcal mol<sup>-1</sup>, in the calculated differential between the ring-bound and O-bound sites.

There is no particular reason to think that the larger basis (“C” basis) gives a better calculation of the absolute binding energies, since our previous experience with the MPW1PW91 functional has given no indication that ring-binding energies calculated with smaller, singly polarized basis sets are systematically low compared with experiment.<sup>13</sup> The present comparison of basis sets shown in Table 1 is a reminder that there is a variation of 1 or 2 kcal mol<sup>-1</sup> in DFT calculations of such metal/substrate binding energies depending on basis set choices. These variations are, however, less severe than those arising from the choice among different well-regarded hybrid density functionals, and should be regarded as an inevitable part of the inherent level of uncertainty of such DFT calculations.

Corrections were applied for both zero-point vibrational energy effects (ZPVE) and basis-set superposition errors (BSSE) (both of which act to reduce the calculated binding energies). Both of these corrections were small and highly consistent across the entire series. ZPVE corrections were calculated for all cases with vibrational frequencies at the level of the “A” basis set. For ring-bound complexes the ZPVE corrections were of magnitude 0.47 ± 0.15 kcal mol<sup>-1</sup>, and for O-bound complexes 0.32 ± 0.08 kcal mol<sup>-1</sup>. BSSE corrections were calculated according to the geometry-consistent procedure described by Xantheas<sup>39</sup> for representative subsets of binding energies, giving an average correction of 0.5 ± 0.1 kcal mol<sup>-1</sup> (9 values) for the “B” basis and 0.4 ± 0.1 kcal mol<sup>-1</sup> (7 values) for the “C” basis. Since the BSSE corrections were both small and nearly constant, it was not considered necessary to calculate the whole set; instead, these average values were applied to all complexes.

## Results

**RAK Experimental Results.** Experiments were undertaken for the transition metal series from Sc<sup>+</sup> to Cu<sup>+</sup>. For the purposes of this study, the observations on the early transition metal ions Ti<sup>+</sup> and V<sup>+</sup> were unsuccessful. The only peaks observed in the

mono complex region attributable to M<sup>+</sup> chemistry corresponded to the additions of *m/z* 42, corresponding apparently to the formation of M<sup>+</sup>(C<sub>2</sub>H<sub>2</sub>O). The reactions forming this species were fast, as would be expected for exothermic bimolecular elimination reactions. As no metal-ion association products were obtained to allow kinetic characterization of reaction 1, these metals were not studied further. Sc<sup>+</sup> appeared to undergo rapid chemistry leading to a large peak at the mass of the bis complex, but no mono complex could be observed. It appears that the mono complex reacted so fast to give bis complex that only the latter could be seen. The Sc<sup>+</sup> spectra obtained had poor quality, and we did not try to resolve the kinetics.

With Mn<sup>+</sup> no reaction could be observed at the limit of detectability. This is consistent with the expected low Mn<sup>+</sup> affinity of furan. Cr<sup>+</sup> was also expected to give slow association, which would make observation of the complex difficult, but sufficient association product was obtained to determine a rate constant. The remaining late transition metal ions, Fe<sup>+</sup> to Cu<sup>+</sup>, gave more or less rapid association reactions, as shown in Table 2. The association rate constant for Fe<sup>+</sup> was an order of magnitude lower than that reported by Bakhtiar and Jacobson,<sup>30</sup> but their experiments, conducted with a high pressure of Ar gas, very likely measured collision-stabilized association rather than radiative association, and are thus probably not comparable to the present low-pressure work.

Co<sup>+</sup> and Ni<sup>+</sup>, in addition to the simple association product, showed a competing bimolecular CO elimination reaction,



with a branching ratio of about 1.5:1 for reaction 2 versus reaction 1 in both cases. The effect of such a competing reaction channel on the association reaction kinetics is complicated in general. However, the reasonable assumption that the reaction involves reactant ions mainly at the upper end of the thermal spread of ion energies gives a simplification that makes possible a straightforward data analysis. Following this idea, it was assumed that the competing product channel (reaction) repre-

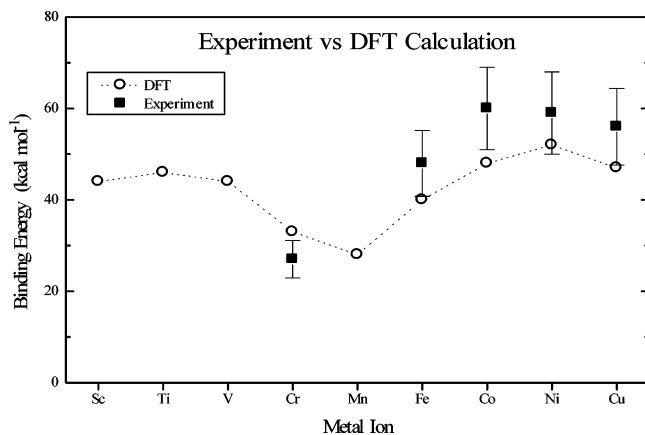


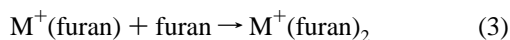
**Figure 1.** Experimental and DFT computational values for M<sup>+</sup>/furan binding energies. Calculated results from Table 1, ring-bound structure, basis "C". Experimental values from Table 1.

sents a reaction of the fraction of the reactants having sufficient thermal excitation to overcome a small activation barrier and proceed to a rearranged product, with CO elimination. The simplifying approximation can then be made that the fraction of the reactants undergoing reaction 2 were probably relatively high in internal energy such that they would have been unlikely to be radiatively stabilized to give stable M<sup>+</sup>(furan), even if reaction 2 had not been available to them. Accordingly, it was considered that the observed rate of formation of stable M<sup>+</sup>(furan) was a valid measure of the intrinsic rate of radiative association, and that no correction was necessary to account for the possible effect of the competing reaction on the association kinetics.<sup>40</sup>

The RAK binding energy results obtained with use of VTST analysis of the kinetics of formation of mono complexes are shown in Table 2, along with corresponding results from the previous pyrrole study. The rate constants are seen to be somewhat lower in the furan reactions compared with corresponding pyrrole cases. Part of this difference arises from the fact that the furan complex has fewer degrees of freedom (by three) than the pyrrole complex, but the full VTST analysis shows that these relative rate constants also imply substantially weaker bond strengths for the furan cases. Thus the RAK experimental binding energies assigned for furan shown in Table 2 are consistently lower than those to the corresponding metals for pyrrole. The RAK experiment comparisons in Table 1 give strong experimental confirmation to the conclusion that pyrrole is a stronger binder of late transition metal ions than furan.

The furan experimental results are also plotted in Figure 1 along with the DFT calculated values. From both Table 1 and Figure 1 it is seen that the RAK results for the late transition metal ions are consistently higher than the DFT calculated values.

All of the cases where reaction 1 was observed to give stable mono complexes (Cr<sup>+</sup>, Fe<sup>+</sup>, Co<sup>+</sup>, Ni<sup>+</sup>, and Cu<sup>+</sup>) also showed the further sequential reaction to give bis complexes,



The bis complex formation rate constants were qualitatively slower (by factors of about 2 to 10) than the corresponding pyrrole values. Because the smaller size of furan leads to an expectation of slower rates than pyrrole, this observation suggests bis complex binding energies not greatly different from those previously assigned for the pyrrole bis complexes. No quantitative assignments of the kinetics or the binding energies

of the bis complexes were carried out. Fe<sup>+</sup> also showed significant formation of the ion at *m/z* 174 representing formal loss of H<sub>2</sub>O from the bis complex.

## Computational Results

The binding of this set of metal ions to benzene-like  $\pi$  rings has received a good deal of careful theoretical consideration. Benzene was discussed in the foundational papers of Bauschlicher et al.,<sup>41,42</sup> and with further consideration and experimental results from the Armentrout group.<sup>32</sup> The effects governing transition metal ion binding to aromatic as well as other types of electron-donating ligands have been developed in particularly careful detail and applied to thermochemical studies of numerous gas-phase systems by the Armentrout and Rodgers groups (see ref 43, for example). The pyrrole system, which is closely similar to the furan system, was carefully considered by Gapeev et al.<sup>3</sup> The present analysis is quite parallel to the pyrrole analysis. Gapeev et al. calculated energies for many of the numerous excited electronic states of the complexes arising from different d-orbital configurations and spin pairings. It did not seem important to repeat this process for all the states of the furan complexes. In the present work, the possible d-orbital configurations and spin states were explored with sufficient care to identify the ground-state configuration and spin with confidence, and the geometry optimization and energy calculations were then carried out for these ground states. Table 3 displays the ground-state geometrical properties calculated for these complexes.

Na<sup>+</sup> with its fully closed shell is considered to be bound electrostatically as a spherical charge. Mg<sup>+</sup> is generally found to be very similar in its  $\pi$  binding to Al<sup>+</sup>. The electron in the HOMO of Mg<sup>+</sup> occupies an orbital of basically 3s character, but there is significant s/p hybridization: an admixture of about 15% p character polarizes the s electron density away from the ring by an important amount, minimizing the nonbonding repulsion. The doubly occupied s orbital of Al<sup>+</sup> is similarly polarized, although to a slightly lesser extent. The greater repulsion resulting from the doubly occupied s orbital is compensated by the smaller size of Al<sup>+</sup>, resulting in virtually identical binding distance and binding energies for Al<sup>+</sup> and Mg<sup>+</sup>. All three of these main-group ions bind  $\eta^5$  essentially over the center of the furan ring.

Just as was found for pyrrole, the early transition metals (Sc<sup>+</sup> to V<sup>+</sup>) bind more or less over the center of the ring ( $\eta^5$ ), as does Mn<sup>+</sup>. This may be thought of as resulting from the relatively large size of the electron clouds of these ions, which presumably tends to fill up the broad potential energy trough above the ring. (In the case of Mn<sup>+</sup>, which is intrinsically smaller than Cr<sup>+</sup> due to its higher nuclear charge, the large effective size of the monocation results from the fact that the outermost electron occupies an essentially 4s orbital, rather than a 3d orbital as is the case for the other transition metal ions in these complexes.) The later transition metals all show a tendency to move away from the heteroatom and to coordinate to more restricted numbers of carbons on the opposite side of the ring. Two patterns are seen: Cr<sup>+</sup>, Ni<sup>+</sup>, and Cu<sup>+</sup> remain on the vertical symmetry plane of the furan ring, with apparently  $\eta^2$  coordination of the two opposite carbons (although for Ni<sup>+</sup> the displacement is not so large as to make it clear whether to call this case  $\eta^2$  rather than  $\eta^4$  or  $\eta^5$ ). Fe<sup>+</sup> and Co<sup>+</sup> move off of the symmetry plane to a position essentially directly over one of the opposite carbons, with apparent  $\eta^1$  coordination. These geometries are quite similar to those described for pyrrole, except that in the pyrrole study, the metal ion was not observed

**TABLE 3: Geometrical Parameters Calculated for the Minimum-Energy Binding Structures of Metal-Ion/Furan Ring-Bound Complexes**

	Na	Mg	Al	Sc	Ti	V	Cr	Mn	Fe	Co	Ni	Cu
				ring bound								
ring-plane-to-metal distance (Å)	2.51	2.39	2.39	2.11	1.96	2.11	2.26	2.41	2.06	1.96	1.93	2.04
metal displacement (Å) <sup>a</sup>	-0.04	0.22	-0.19	-0.37	-0.18	0.12	0.7	0.21	0.64 <sup>b</sup>	0.47 <sup>b</sup>	0.47	1.03
apparent coordination	$\eta^5$	$\eta^5$	$\eta^5$	$\eta^5$	$\eta^5$	$\eta^5$	$\eta^2$	$\eta^5$	$\eta^{1b}$	$\eta^{1b}$	$\eta^2$	$\eta^2$
				O bound								
oxygen-to-metal distance (Å)	2.14	2.09	2.09	2.19	2.04	2.10	2.10	2.19	2.02	1.99	1.96	1.95

<sup>a</sup> Displacement of the metal ion from the position over the geometrical center of the ring, in the direction away from the O atom. The position over the O atom is at  $-1.29$  Å, while the position directly on top of the opposite edge of the ring is at a position of  $0.99$  Å. <sup>b</sup> In these  $\eta^1$  cases the metal ion is displaced away from the vertical symmetry plane of furan, and lies essentially on top of one of the carbon atoms.

to shift away from the symmetry plane to give  $\eta^1$  binding sites for  $\text{Fe}^+$  and  $\text{Co}^+$  like those found here for furan. It should be noted that the potential energy surface above these rings is quite flat, so that there is generally quite a small energy cost of moving a metal ion around to give various types of binding sites as described here.

In contrast to the rather free lateral movement of the metal ion over the ring, the distance of a particular metal ion above the ring is more tightly constrained. The ring-to-metal distances calculated for furan do not differ from those described for benzene and pyrrole in ways that seem significant.

## Discussion

**Prior Results.** The present results can be compared with the various prior furan results noted above. Stöckigt<sup>38</sup> assigned an  $\text{Al}^+$ /furan binding energy of  $29.2$  kcal mol<sup>-1</sup> based on calculations by a number of different approaches. This is in very satisfactory agreement with the present results. For  $\text{Fe}^+$ , the range of  $38.5$  to  $60$  kcal mol<sup>-1</sup> from Bakhtiar and Jacobson<sup>30</sup> comfortably accommodates both our experimental and computed values ( $48$  and  $46$  kcal mol<sup>-1</sup>, respectively). For  $\text{Co}^+$ , the upper limit of  $60$  kcal mol<sup>-1</sup> of Nanayakkara and Freiser<sup>27</sup> does not contradict either our experimental ( $61 \pm 9$  kcal mol<sup>-1</sup>) or our computed ( $48$  kcal mol<sup>-1</sup>) values, and their best value of  $57$  kcal mol<sup>-1</sup> compares well with our results. Moreover, we agree with their conclusion that pyrrole is a stronger ligand for  $\text{Co}^+$  than furan. For  $\text{Ni}^+$ , the estimate of  $50$  kcal mol<sup>-1</sup> from Kappes and Staley<sup>31</sup> is in satisfactory agreement with the present computed value ( $52$  kcal mol<sup>-1</sup>) and somewhat lower than the present experimental determination ( $59 \pm 9$  kcal mol<sup>-1</sup>), although easily within the uncertainty.

Thus for the three late transition metal ions  $\text{Fe}^+$ ,  $\text{Co}^+$ , and  $\text{Ni}^+$ , the present results are consistent with previous information. The substantial uncertainty of our RAK assignments, and the unknown quality of the absolute binding energies from DFT calculations, limit the extent to which the present results improve the situation. For  $\text{Fe}^+$ , they indicate a true value lying in the central part of the broad range given by Bakhtiar and Jacobson.<sup>30</sup> For  $\text{Co}^+$ , they suggest that the value assigned by Nanayakkara and Freiser,<sup>27</sup> which properly speaking was only an upper limit, is not greatly higher than the true value. We would put more confidence in the estimate of Kappes and Staley<sup>31</sup> than in the present absolute assignments for the  $\text{Ni}^+$  complex, but it is good to find no contradiction with their work. The upper limit of  $37$  kcal mol<sup>-1</sup> on the  $\text{Cu}^+$ (furan) binding energy from threshold photodissociation<sup>29</sup> seems too low based on the present results. Both unrecognized internal excitation of the ions and unrecognized multiphoton dissociation can lead to erroneously low dissociation energies from this technique,<sup>17</sup> so it seems likely that this binding energy is actually higher than their value. Direct measurement of the  $\text{M}^+$ /furan dissociation energies by a

dissociation technique seems necessary for more confident assignment of the absolute binding thermochemistry in these systems than the rather loose ranges given by previous work and the present results.

**Agreement of Computation and Experiment.** The agreement of the RAK experimental results with the calculations is less good than might be hoped, although, with the generous but probably realistic error bars placed on the RAK values, the disagreements are not outside the combined uncertainties. The measured radiative association rates were faster than expected from the calculated binding energies. A similar disagreement was reported for pyrrole, where radiative association was found to be faster than expected for  $\text{Fe}^+$ , and particularly  $\text{Co}^+$  and  $\text{Ni}^+$ , corresponding to binding energies higher than calculated. However, in comparing the pyrrole study to the present furan work, it should be noted that the previous pyrrole calculations used the B3LYP functional which we now consider to underestimate the binding energies, so the agreement of theory and experiment would improve for pyrrole if it were treated in the same way as we have treated furan.

The acceptable agreement found between experiment and theory gives reassurance that the calculations were performed for appropriate geometries and electronic states of the complexes. This being true, it seems likely that DFT calculations on simple systems such as these will have better precision than the RAK experimental binding energies, which have rather large uncertainties. Accordingly, the DFT results will be taken as the basis for the following comparisons and discussion of systematic trends.

**Binding Mechanisms.** It is helpful to consider the binding of metal ions as composed of three types of interactions: (1) the pure electrostatic interaction of the positive charge of the ion with the charge distribution of the isolated molecule; (2) the polarization interaction of the ionic charge with the induced charge distribution of the molecule sitting in the electric field of the ion, which is traditionally, though inaccurately, called the “charge-induced-dipole interaction” (note that polarization binding is defined in some of the literature as part of the “electrostatic” binding, but we favor using the latter term to refer specifically to the static charge-multipole interactions); and (3) electronic effects, which can be described as orbital overlap and mixing, orbital hybridization, charge transfer, closed-shell repulsions, and so forth.

In developing a qualitative understanding of the trends observed in the present series, we can take the point of view that the polarization part of the binding, while large, does not vary much when comparing a given metal ion’s binding to these three ligands in a similar  $\pi$ -binding geometry over the aromatic ring. It is true that the distance from the rings varies somewhat for the different ligands. Benzene<sup>13</sup> is on the average  $0.07$  Å closer to the metal than furan, and  $0.03$  Å closer than pyrrole.<sup>3</sup>

**TABLE 4: Electrostatic Potential Energy Well Depth and Position Calculated for Cation Binding over the  $\pi$  Face**

	well depth (kcal mol <sup>-1</sup> )	height above ring plane (Å)	lateral displacement from ring center (Å)
benzene	-17.2	1.89	
pyrrole	-27.5 <sup>a</sup>	1.72	0.97
furan	-15.4	1.90	0.83

<sup>a</sup> The electrostatic potential energy minimum for pyrrole is closer to the ring than for the other two molecules, as shown in the table. However, this difference in electrostatically preferred binding geometry is not likely to be important to the actual binding, because it costs only 1.5 kcal of electrostatic energy to move the cation away from the pyrrole ring to a distance of 1.90 Å similar to the other systems. This is a small amount of energy in comparison with other factors governing the binding thermochemistry and geometry.

Other things being equal, such a difference in distance could give a relatively minor variation of the polarization energy of the order of 1–2 kcal mol<sup>-1</sup> according to simple model calculations, but the situation is actually too complicated to evaluate with any simple model. We will not explore this question further, beyond assuming that the three ligands have similar polarization contributions. The rest of this subsection considers the systematic comparison of the electrostatic binding contributions between benzene, pyrrole, and furan. After that, a few points are made about the electronic interactions, although a complete dissection and analysis of the binding is not attempted in this paper.

The electrostatic component of binding to these  $\pi$  faces arises from the accumulation of net negative charge in the  $\pi$  system. This creates a region of negative potential energy above the ring for interaction of the cation with the electronic cloud of the molecule. This is the same as saying that there is an accumulation of excess negative charge above the ring in the region where cation binding takes place, and is also similar to describing the electrostatic binding of cations to these systems in terms of a favorable charge-quadrupole interaction. Qualitatively, one can gain insight into the comparison of the heteroatom systems with benzene by looking at the variations in this electrostatic potential well. Since the electrostatic potential energy surface is available from the computed electron density of the neutral molecule, the electrostatic potential energy surface and the desired potential energy well for cation interaction are immediately available from the computed DFT results. Table 4 shows the depth and location of the electrostatic potential well for the three systems.

Compared with benzene, both of the heteroaromatic molecules differ in that two of the six  $\pi$  electrons are supplied by the  $p_z$  atomic orbital of the heteroatom. These two  $\pi$  electrons delocalize around the ring, which tends to give a shift of electron density away from the heteroatom and into the region of cation- $\pi$  binding. Compensating for this effect, the heteroatom has higher electronegativity than carbon, which tends to shift electron density away from the  $\pi$  cloud. For pyrrole, the first of these effects dominates, and it is seen (Table 4) that the electrostatic potential energy well is deeper by several kcal mol<sup>-1</sup> than for benzene. For furan, the high oxygen electronegativity leads to the domination of the second of these effects, and the potential energy well is shallower than for benzene. This contrast also shows up in the total Mulliken populations of the heteroatoms: the N atom in pyrrole is actually positive, with a net charge of 0.06, while the O atom of furan is negative, with a net charge of -0.11. For both heteroatom systems the shift of excess  $\pi$  electron density away from the heteroatom is seen in the fact that the center of the  $\pi$  potential energy well for both pyrrole and furan is shifted substantially away from

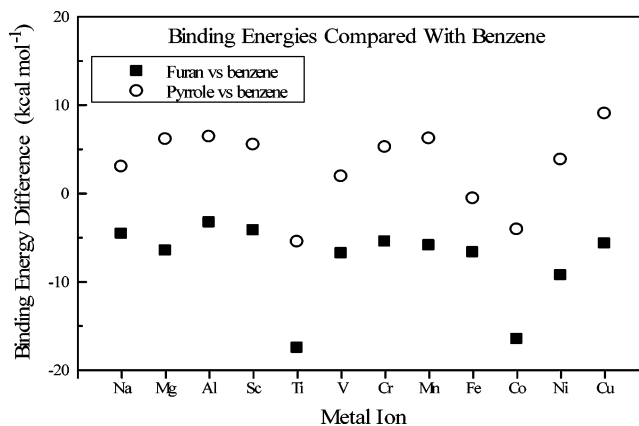


**Figure 2.** Cation- $\pi$  binding energy differentials for heteroatom ligands versus benzene (binding energy to ligand minus binding energy to benzene). Furan results are present DFT/MPW1PW91 results. Pyrrole results are from DFT calculations in ref 3, using the B3LYP functional.

the geometrical center of the ring in the direction away from the heteroatom.

This analysis gives a context for interpreting the comparisons displayed in Figure 2, where it is seen that binding is stronger by  $\sim 5$  kcal mol<sup>-1</sup> to pyrrole than to benzene, while binding is weaker by  $\sim 5$  kcal mol<sup>-1</sup> to furan than to benzene. This is completely consistent with the direction, and approximate magnitudes, predicted by the electrostatic comparisons of Table 4. Our interpretation is that the polarization effects and the specific orbital-interaction effects are nearly the same for benzene and the other cases. This makes the relatively small differences in the molecular electrostatic potential energy wells clearly discernible, even though the absolute binding energies vary from metal to metal by large amounts.

Within this context, two transition metal ions, Ti<sup>+</sup> and Co<sup>+</sup>, stand out in Figure 2 as notable exceptions. Each of these shows much stronger binding to benzene relative to the other systems than would be expected in terms of the electrostatic binding argument. This presumably reflects particular characteristics of the d-orbital interactions in these cases, such that for these particular two metal ions binding to benzene is specifically enhanced relative to both of the heteroatom systems. The reasons for this are not clearly established. Co<sup>+</sup> is clearly unusual. Its binding with benzene is distinctly stronger than that to its neighbors Fe<sup>+</sup> and Ni<sup>+</sup>, but this is not the case for furan; the relatively less favorable binding in the furan case is also suggested by this ion's choice of an  $\eta^1$  binding geometry in preference to more delocalized interaction with the ring  $\pi$  system. The anomalous thermochemistry of Ti<sup>+</sup> binding is even harder to account for. Its binding geometry to furan and pyrrole shows the normal delocalized  $\eta^5$  pattern similar to benzene, and the orbital occupations of the d orbitals are identical for the three ligands. Yet, for no obvious reason, binding to benzene is calculated to be much stronger than expected relative to the heteroatom systems. This is not a peculiarity of the MPW1PW91 functional, since very similar trends are found by using the B3LYP functional. It may be an artifact of the DFT method in general, or it may reflect a specific effect of the d-orbital interactions that is not yet understood. Both of these exceptional cases have in common the fact that the valence d shell has three electrons outside of filled (and half-filled) orbital shells. This gives complicated electron-coupling situations and multiple possible spin states. These are thus among the most difficult systems to calculate, and it is not surprising to find them behaving in ways that are not fully understood.

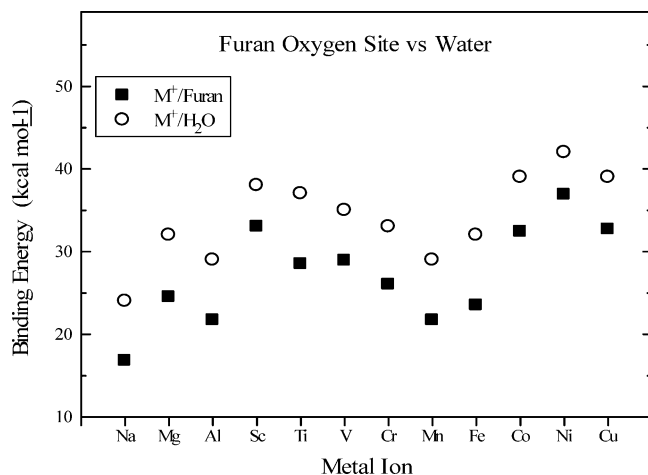


**Figure 3.** Comparison of O-site binding energies on furan with H<sub>2</sub>O binding energies from ref 13. All values are DFT/MPW1PW91. For best comparability, the furan results from Table 1 are the “A” basis values. The Fe<sup>+</sup>/H<sub>2</sub>O value from ref 13 has been corrected by 5.7 kcal mol<sup>-1</sup> to agree with the present protocol.

**Oxygen Site.** A natural comparison can be made between binding to the oxygen lone-pair site of furan, which might be affected by the aromatic character of the oxygen, and binding to a normal divalent oxygen, like that in water. Figure 3 shows this comparison, and it is clear that the binding energies of these two types of oxygen sites are closely parallel across the periodic series. The furan oxygen site is consistently less strongly bound than the water site. There are strong binding energy effects for oxygen sites depending on the metal-ion type and the d-electron configurations of the transition metals, as was discussed and explained in detail in the original H<sub>2</sub>O study of Bauschlicher et al.<sup>42,44</sup> However, these effects appear to be identical for water and furan, within a reasonable degree of scatter, and we conclude that the nature of binding to the oxygen in-plane lone pair is similar in character, although not in absolute strength, for the oxygens in these two different environments. The furan site is on the average  $6.7 \pm 1.6$  kcal mol<sup>-1</sup> weaker than the water site, for corresponding metal ions. Electrostatic effects are probably the principal reason for this difference, although the polarization contributions are also expected to be different between water and furan. As a rough indicator of the electrostatic contributions to the oxygen-site binding, the electrostatic potential energy is calculated to be  $-28$  kcal mol<sup>-1</sup> for water, and only  $-15$  kcal mol<sup>-1</sup> for furan, at a distance of 2.0 Å away from the oxygen; this difference is more than sufficient to rationalize stronger binding to water than to furan.

A principal goal of the computational part of this work was to assess the relative binding abilities of the two sites on furan. This comparison is shown in Figure 4. Two main points can be made. First, the oxygen site in this system is definitely weaker than the  $\pi$  site for all metal ions, even those for which electronic effects involving the transition metal d orbitals are small. The main-group metals without d-orbital contributions, Na<sup>+</sup>, Mg<sup>+</sup>, and Al<sup>+</sup>, show ring binding stronger than O binding by an amount of the order of 5 kcal mol<sup>-1</sup>. This is also the case for Cr<sup>+</sup> and Mn<sup>+</sup>, where d electrons are present as a spherically symmetric half-closed shell, giving little d-orbital-based binding enhancement. Cu<sup>+</sup>, with a fully filled d shell, might be expected to be similar to these, but actually, as is true for Cu<sup>+</sup> in other  $\pi$ -binding situations, it shows a considerably greater preference for ring binding than expected on this basis.

The second point drawn from Figure 4 is that the metal ions with partially filled d-orbital shells, namely Sc<sup>+</sup>, Ti<sup>+</sup>, V<sup>+</sup>, Fe<sup>+</sup>,

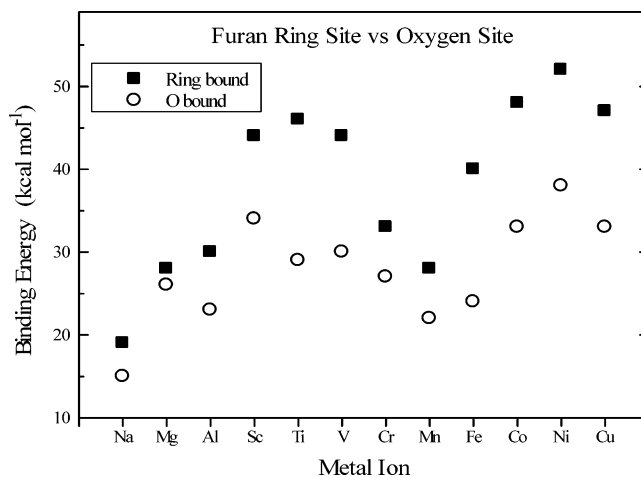


**Figure 4.** Comparison of the two binding sites on furan. Binding energies from Table 1 (“C” basis).

Co<sup>+</sup>, and Ni<sup>+</sup>, all show greatly enhanced ring binding compared with oxygen binding, with a ring binding preference of the order of 15–20 kcal mol<sup>-1</sup>. The electron-donation and back-donation effects between the metal d orbitals and the ligand  $\pi$  and  $\pi^*$  orbitals leading to this highly favorable binding to the cyclic  $\pi$  system are well understood.<sup>41–43</sup>

In the case of phenol,<sup>13</sup> it was considered that only for Na<sup>+</sup>, and perhaps Mg<sup>+</sup>, is there likely to be a significant fraction of the population having metal ion bound to the oxygen site in competition with the ring site under thermally equilibrated conditions. The furan system shows even less relative metal-ion affinity for the oxygen site than phenol, and it seems unlikely that this site is thermally accessible for any of these metal cations binding to furan.

## Conclusions

Furan as a  $\pi$  binding site for transition metal monocations has been examined by both experimental and computational methods. Experimental results for five metal-ion systems confirm the order and relative values of the corresponding computed values. Given the substantial uncertainty of these experiments, the computed values are probably better estimates of the absolute binding energies.

These results confirm that furan is indeed a  $\pi$ -bonding ligand closely parallel to benzene and pyrrole. Its lower  $\pi$ -affinity for metal ions relative to these others is easily attributable to the lower electrostatic contribution to the overall binding, resulting from the withdrawal of electron population from the  $\pi$  system by the electronegative oxygen heteroatom. The parallel patterns of binding energies of these three systems going across the metal-ion series suggest very similar electronic interactions. Just as with pyrrole, the late transition metals show large displacements away from the center of the ring, but this does not alter the pattern of  $\pi$ -to-d donations and d-to- $\pi^*$  back-donations that was laid out by Bauschlicher et al.<sup>41,42</sup> to account for the periodic trends in binding energies. The tendency of the late transition metal ions (as well as Cr<sup>+</sup>) to move away from the ring center to a lower coordinating position than  $\eta^5$  may provide a way to reduce the repulsive interactions between the ring  $\pi$  orbitals and the occupied d orbitals having unfavorable shape<sup>43</sup> (although this simple argument does not account for the Fe<sup>+</sup> case).

In the series of four ligands laid out in the Introduction, furan is unique in having both well defined  $\pi$  and n-donor binding sites, but nevertheless preferring  $\pi$  complexation of metal cations. This preference is modest but clear for the metal ions



that do not have major d-orbital participation in the binding, and becomes large for transition metal ions with favorable interactions of the d and  $\pi$  systems. Furan is a slightly weaker cation- $\pi$  binding ligand than benzene for both main-group and transition metal cations.

**Acknowledgment.** The support of the National Science Foundation and of the donors of the Petroleum Research Fund, administered by the American Chemical Society, is acknowledged.

## References and Notes

- (1) Ma, J. C.; Dougherty, D. A. *Chem. Rev.* **1997**, *97*, 1303.
- (2) DeWall, S. L.; Meadows, E. S.; Barbour, L. J.; Gokel, G. W. *Proc. Natl. Acad. Sci. U.S.A.* **2000**, *97*, 6271.
- (3) Gapeev, A.; Yang, C.-N.; Klippenstein, S. J.; Dunbar, R. C. *J. Phys. Chem. A* **2000**, *104*, 3246.
- (4) Rodgers, M. T.; Stanley, J. R.; Amunugama, R. *J. Am. Chem. Soc.* **2000**, *122*, 10969.
- (5) Groyzman, S.; Goldberg, I.; Kol, M.; Genizi, E.; Goldschmidt, Z. *Organometallics* **2003**, *22*, 3013.
- (6) Rothermel, G. L., Jr.; Miao, L.; Hill, A. L.; Jackels, S. J. *Inorg. Chem.* **1992**, *31*, 4854.
- (7) Hu, J.; Barbour, L. J.; Gokel, G. W. *Chem. Commun.* **2002**, 2002.
- (8) Hu, J.; Barbour, L. J.; Ferdani, R.; Gokel, G. W. *Chem. Commun.* **2002**, 2002, 1810.
- (9) Oomens, J.; Moore, D. T.; von Helden, G.; Meijer, G.; Dunbar, R. C. *J. Am. Chem. Soc.* **2004**, *126*, 724.
- (10) Lemaire, J.; Boissel, P.; Heninger, M.; Mauclair, G.; Bellec, G.; Mestdagh, H.; Simon, A.; LeCaer, S.; Ortega, J. M.; Glotin, F.; Maitre, P. *Phys. Rev. Lett.* **2002**, *89*, 273002.
- (11) LeCaër, S.; Heninger, M.; Lemaire, J.; Boissel, P.; Maitre, P.; Mestdagh, H. *Chem. Phys. Lett.* **2004**, *385*, 273.
- (12) Kapota, C.; Lemaire, J.; Maitre, P.; Ohanessian, G. *J. Am. Chem. Soc.* **2004**, *126*, 1836.
- (13) Dunbar, R. C. *J. Phys. Chem. A* **2002**, *106*, 7328.
- (14) Gapeev, A.; Dunbar, R. C. *Int. J. Mass Spectrom.* **2003**, *228*, 825.
- (15) Ryzhov, V.; Dunbar, R. C. *J. Am. Soc. Mass Spectrom.* **1999**, *10*, 862.
- (16) Bartmess, J. E. Bracketing. In *Encyclopedia of Mass Spectrometry; Chemistry and Physics of Gas-Phase Ions*; Armentrout, P. B., Ed.; Elsevier: Oxford, UK, 2003; Vol. 1, p 315.
- (17) Dunbar, R. C. Photodissociation Studies of Ion Thermochemistry. In *Encyclopedia of Mass Spectrometry; Chemistry and Physics of Gas-Phase Ions*; Armentrout, P. B., Ed.; Elsevier: Oxford, UK, 2003; Vol. 1, p 403.
- (18) Armentrout, P. B. *Acc. Chem. Res.* **1995**, *28*, 430.
- (19) Cooks, R. G.; Patrick, J. S.; Kotiaho, T.; McLuckey, S. A. *Mass Spectrom. Rev.* **1994**, *13*, 287.
- (20) Dunbar, R. C. Radiative Association Kinetics: Ion-Ligand Binding Thermochemistry. In *Encyclopedia of Mass Spectrometry; Chemistry and Physics of Gas-Phase Ions*; Armentrout, P. B., Ed.; Elsevier: Oxford, UK, 2003; Vol. 1, p 362.
- (21) Stöckigt, D.; Hrušák, J.; Schwarz, H. *Int. J. Mass Spectrom. Ion Proc.* **1994**, *149/150*, 1.
- (22) Dunbar, R. C.; Klippenstein, S. J.; Hrušák, J.; Stöckigt, D.; Schwarz, H. *J. Am. Chem. Soc.* **1996**, *118*, 5277.
- (23) Ryzhov, V.; Yang, C.-N.; Klippenstein, S. J.; Dunbar, R. C. *Int. J. Mass Spectrom.* **1999**, *185/186/187*, 913.
- (24) Gapeev, A.; Dunbar, R. C. *J. Phys. Chem. A* **2000**, *104*, 4084.
- (25) Gapeev, A.; Dunbar, R. C. *J. Am. Soc. Mass Spectrom.* **2002**, *13*, 477.
- (26) Huang, H.; Rodgers, M. T. *J. Phys. Chem. A* **2002**, *106*, 4277.
- (27) Nanayakkara, V. K.; Freiser, B. S. *J. Mass Spectrom.* **1997**, *32*, 475.
- (28) Su, P.-H.; Yeh, C.-S. *Chem. Phys. Lett.* **2000**, *331*, 420.
- (29) Su, P. H.; Lin, F. W.; Yeh, C. S. *J. Phys. Chem. A* **2001**, *105*, 9643.
- (30) Bakhtiar, R.; Jacobson, D. B. *J. Am. Soc. Mass Spectrom.* **1996**, *7*, 938.
- (31) Kappes, M. M.; Staley, R. H. *J. Am. Chem. Soc.* **1982**, *104*, 1813.
- (32) Meyer, F.; Khan, F. A.; Armentrout, P. B. *J. Am. Chem. Soc.* **1995**, *117*, 9740.
- (33) Surya, P. I.; Roth, L. M.; Ranatunga, D. R. A.; Freiser, B. S. *J. Am. Chem. Soc.* **1996**, *118*, 1118.
- (34) Dunbar, R. C. *Int. J. Mass Spectrom. Ion Proc.* **1997**, *160*, 1.
- (35) Bartmess, J. E.; Georgiadis, R. M. *Vacuum* **1983**, *33*, 149.
- (36) Klippenstein, S. J.; Yang, Y.-C.; Ryzhov, V.; Dunbar, R. C. *J. Chem. Phys.* **1996**, *104*, 4502.
- (37) Frisch, M. J.; Trucks, G. W.; Schlegel, H. B.; Scuseria, G. E.; Robb, M. A.; Cheeseman, J. R.; Zakrzewski, V. G.; Montgomery, J. A., Jr.; Stratmann, R. E.; Burant, J. C.; Dapprich, S.; Millam, J. M.; Daniels, A. D.; Kudin, K. N.; Strain, M. C.; Farkas, O.; Tomasi, J.; Barone, V.; Cossi, M.; Cammi, R.; Mennucci, B.; Pomelli, C.; Adamo, C.; Clifford, S.; Ochterski, J.; Petersson, G. A.; Ayala, P. Y.; Cui, Q.; Morokuma, K.; Malick, D. K.; Rabuck, A. D.; Raghavachari, K.; Foresman, J. B.; Cioslowski, J.; Ortiz, J. V.; Stefanov, B. B.; Liu, G.; Liashenko, A.; Piskorz, P.; Komaromi, I.; Gomperts, R.; Martin, R. L.; Fox, D. J.; Keith, T.; Al-Laham, M. A.; Peng, C. Y.; Nanayakkara, A.; Gonzalez, C.; Challacombe, M.; Gill, P. M. W.; Johnson, B.; Chen, W.; Wong, M. W.; Andres, J. L.; Gonzalez, C.; Head-Gordon, M.; Replogle, E. S.; Pople, J. A. *Gaussian 98*, Revision A.6; Gaussian, Inc.: Pittsburgh, PA, 1998.
- (38) Stöckigt, D. *J. Phys. Chem. A* **1997**, *101*, 3800.
- (39) Xantheas, S. S. *J. Chem. Phys.* **1996**, *104*, 8821.
- (40) A referee points out the possibility that this competing endothermic reaction could reflect a fraction of electronically excited metal ions, and this can certainly not be ruled out. This explanation would, however, imply that at least 60% of the metal ions were electronically excited for both Co and Ni, which has not generally been thought to be the case under the long-time-scale ion trapping conditions of ICR experiments.
- (41) Bauschlicher, C. W., Jr.; Partridge, H.; Langhoff, S. R. *J. Phys. Chem.* **1992**, *96*, 3273.
- (42) Bauschlicher, C. W., Jr.; Langhoff, S. R.; Partridge, H. Transition metals. In *Organometallic Ion Chemistry*; Freiser, B. S., Ed.; Kluwer Academic Publishers: Dordrecht, The Netherlands, 1996; p 47.
- (43) Rodgers, M. T.; Armentrout, P. B. *Mass Spectrom. Rev.* **2000**, *19*, 215.
- (44) Rosi, M.; Bauschlicher, C. W., Jr. *J. Chem. Phys.* **1989**, *90*, 7264.